Heat Transfer Enhancement using Combined Microchannel with Vertical Rectangular Micro Fins

N. Y. Godi

Department of Mechanical Engineering, Modibbo Adama University, Adamawa State, Nigeria

ABSTRACT: This paper focuses on the numerical optimisation of a combined hybrid microchannel heat sink with rectangular solid fins. The axial length and volume are fixed, and external structure is allowed to vary. The simulation was performed on an elemental unit cell of the microchannel heat sink . The purpose of the optimisation is to discover an optimal geometric arrangement in internal and external configurations that minimises peak temperature in the microchannel heat sink. A high-density uniform heat flux of $250\ \mathrm{W/cm^2}$ is assumed to be dissipated on the bottom wall of the unit cell by microelectronics circuit boards devices. Computational fluid dynamic code was used to discretized the fluid domain and solve a set of governing equations. The influence of hydraulic diameter, external structural shape and fluid velocity on peak temperature and global thermal resistance, is discussed. Coolant or water of Reynolds number range 400 to 500 in a forced convection laminar flow is introduced through the inlet of the computational domain to remove the heat at the bottom of the rectangular block microchannel. The results show that when the fluid velocity is increased from 9.8 to 12.3 m/s across the axial length of the micro heat sink, more heat is removed from the bottom of the combined heat sink. The results revealed that the pump power increased by 37.1% in combined microchannels with fins and from by 27.2% in finless micro heat sink. The result of the study is validated with what is documented in open literature for a traditional micro heat sink with circular flow channel and the trends agree.

KEYWORDS: Microchannel structure, configuration, combined microchannel and micro fins

[Received Nov. 14, 2022; Revised April 4, 2023; Accepted April 14, 2023] Print ISSN: 0189-9546 | Online ISSN: 2437-2110

I. INTRODUCTION

Microchannels have become a phenomenon in heat transfer and thermal management. Microchannel heat sinks account for capacity of high heat dissipation in microelectronics (Gupta *et al*., 2021; Qiu *et al*., 2021; Hajialibabaei and Saghir, 2022). The high heat transfer surface area to volume ratio is what accounts for the excellent thermal efficiency (He, Yan and Zhang, 2021). The design methodology employed in microchannel heat sinks or heat exchangers are based on the heat transfer and pressure drop associated with the device (Han *et al*., 2012). In the construction of most microchannel heat exchangers, each channel is defined by two parallel plates separated by fins or spacers (Kern and Kraus, 1972). The research on microchannel heat exchangers is largely concentrated on the effect of micro heat sink structural forms on efficiency (Chen *et al*., 2021). Heat transfer efficiency and minimum flow resistance of microchannel heat exchangers were experimentally compared for optimised structure with the other three having contrasting arrays of elements under the same constraints. The results of the experiment revealed that the microchannel heat exchanger with optimised structure has a higher thermal performance to flow resistance than the three other structures considered (Chen *et al*., 2021). Khan *et al*. (2022) carried out a numerical analysis on the flow and heat transfer features of microchannel heat sink with perforated pin fin. The performance of the micro heat sink was evaluated within the Reynolds number ranges of 150 to 350 with the six evenly spaced cylindrical pin-fins perforated. The researchers discovered improvement in Nusselt number at the smallest perforation of 0.33 but decreased Nusselt number as the perforation diameter increased. The highest value of overall thermal performance was found to be at the perforation size of 0.5.

Researchers have been conducting numerical studies of microchannels heat exchangers because of the need to provide more viable ways of improving the heat transfer and cooling abilities of electronic devices. The novel work of Tuckerman and Pease (1981) used forced fluid flow through the microchannel heat sink to cool microelectromechanical systems (MEMS).

Heat exchangers are widely used in industries to increase heat transfer. Heat exchangers embrace a diversity of models, shapes and configurations. Most of them are used to enhance the transfer of heat between two flowing mediums at different temperatures. Others consist of a solid cooling or heating system. The heat transfer process in heat exchangers usually

*Corresponding author: nahumgodi@yahoo.co.uk

doi: http://dx.doi.org/10.4314/njtd.v18i4.1454

involves conduction through the solid, and convection between the solid and the fluid. According to Bejan (2016), the very name 'heat exchanger' means that the function of the equipment is to transfer a certain quantity of heat between two or more substances at different temperatures.

In a bid to investigate the constructal law and its usefulness in geometric optimisation, Bello-Ochende *et al*. (2013) performed a numerical and analytical study of square flow channels using a vascularised material having localised internal cooling property with heat flux applied at one side of the heat sink. The goal of the study was to reduce the highest temperature in the material body of the solid substrate. The numerical results revealed that the material property affected the efficiency of the flow channel to a high degree. Salimpour *et al*. (2011) used the constructal approach to numerically optimise different cross-sectional shapes of microchannel. The researchers were able to develop some correlations, which helped in predicting the dimensionless heat transfer and optimal hydraulic diameter. The results of the study revealed that the square shapes had the best heat transfer per unit volume.

Constructal theory is used to geometrically optimise flow architecture and structure for the purpose of increasing heat transfer and fluid flow (Bejan and Dan, 1999; Bejan *et al*., 2000; Rocha *et al*., 2002; Bejan and Fautrelle, 2003; Rocha *et al*., 2005; Kulkarni, 2005; Pramanick, 2007; Reis, 2009; Bello-Ochende *et al*., 2010; Cetkin, 2010; Bello-Ochende *et al*., 2011). The law does not predict flow architecture in advance but allows the system to evolve (Reis, 2006). Bejan and Lorente (2006) reviewed the theory recently and argued that under certain global constraints, the flow architecture should be able to provide little resistance or should increase access to flow. The unit structure that is subject to global constraint and the flow channels' geometric shape are both free to morph. Researchers such as, (Azoumah *et al*., 2007; Wu, Chen and Sun, 2007; Zhou *et al*., 2007; Fan and Luo, 2008; Han *et al*., 2012), have also reported their work on constructal design methodology.

The parts used to extend primary surfaces are referred to as fins. Fins comprise of a vast range of types, shapes and arrangements. In extended surfaces, conduction and convection are most often used for heat transfer, while radiation heat transfer is neglected (Bejan, 1993; Ryu *et al*., 2003). The cooling of electronic equipment using micro pin-fins is gaining attention because of their capacity to dissipate high heat fluxes and improve the thermal management of microelectronic devices. Experimental research using micro pin-fins has revealed that their use in the heat sink increases the heat transfer surface area, reduces to the barest minimum the thermal resistance, reduces space used, lower the mass and cost of the pin-fins (Kim *et al*., 2004). Other researchers, (Koşar *et al*., 2005; Koşar and Peles, 2006; Naphon and Sookkasem, 2007; Siu-Ho *et al*., 2007; John *et al*., 2010; Vilarrubí *et al*., 2018) have also reported their research work on pin-fins of diverse configurations.

Yeh (1997) used an analytic approach to show how the dimension of circular and rectangular micro pin-fins with fixed volume and heat transfer could be maximised. He observed that micro pin-fins with insulated tips had the best aspect ratio with reduced fin volume. Díez *et al*. (2010) reported the effect of roughness on micro pin-fins which were truncated with changing diameter for hyperbolic, trapezoidal and concave parabolic designs. The efficiency and effectiveness of smooth pin-fins, as well as temperature distribution were accurately predicted by the approximate method of truncated power series.

The novelty of the combined constructal design with solid rectangular fins positioned on the block micro-heat sink made from an aluminum substrate to remove heat deposited at the base of the combined micro-heat sink with fins is presented in this paper. Three rows of rectangular micro solid fins are modelled and placed on the heat sink and numerically simulated with water as cooling fluid. The fluid flows through the channel and optimise the internal and external configuration, while cooling the entire system including the solid fins (extended surfaces). Convection heat transfer in the cooling fluid and heat conduction in the solid substrate make up the conjugate solution for heat transport in the computational unit cell. The heat flux and temperature continuity at the solid-fluid interface link between conduction and convection of heat. The study result showed that the combined microchannel has high thermal efficiency and lower pump power than the traditional heat sink without fins.

Nomenclature

A	channel cross-sectional area
d	diameter
d_h	hydraulic diameter
H	height of heat sink
k_f	thermal conductivity of fluid
k_s	thermal conductivity of solid wall
M	width of unit cell micro heat sink
N	axial length of heat sink
n	number of channels
q''	heat flux
Re_w	Reynolds number of water
R_{min}	dimensionless thermal resistance
$T_{w,L}$	exit temperature
T_{in}	inlet temperature
T_{max}	maximum temperature
t_1	distance from bottom to channel
t_2	distance from the top micro heat sink to channel
t_3	channel to channel thickness
v_{in}	inlet velocity
V	volume
v_{el}	elemental volume

Greek symbols

α	thermal diffusivity
C_p	specific heat
μ	viscosity
ν	kinematic viscosity
ρ	density
ϕ	volume fraction of solid material
τ	shear stress

Subscripts

in	inlet
max	maximum
min	minimum
opt	optimum
out	outlet

II. GEOMETRY DESCRIPTION AND COMPUTATIONAL DOMAIN

The constructal physical models of a hybrid (this means having a circular cooling channel, but rectangular micro-fins added) microchannel heat sink is presented in Figures 1 and 2. In Figure 1, rectangular fins are placed on the rectangular block microchannel with circular flow channel of global fixed volume$NxHxM_x$. The geometric design is aimed at finding the design that gives optimal thermal efficiency, using constructal design technique. The coolant used is water and the heat transfer is a conjugate.

Figure 1 shows the diagram of a constructal rectangular block microchannel heat sink with solid rectangular fins mounted on it. Figure 2 is a unit cell symmetrical geometry with three (3) rows of rectangular micro-fins to serve as the computational domain. The volume of the elemental unit cell is given as $N \times H \times M$. The hydraulic diameter d_h is surrounded by solid material structure with thicknesses t_1, t_2 and t_3.

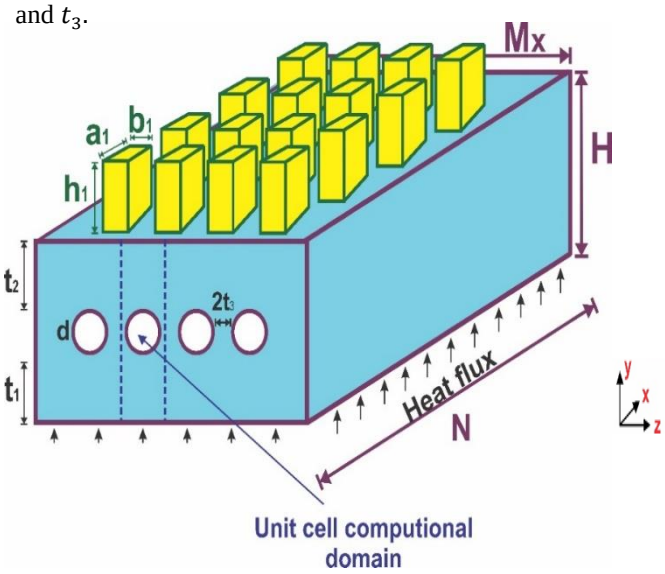

Figure 1: Microchannel heat sink with rectangular solid fins

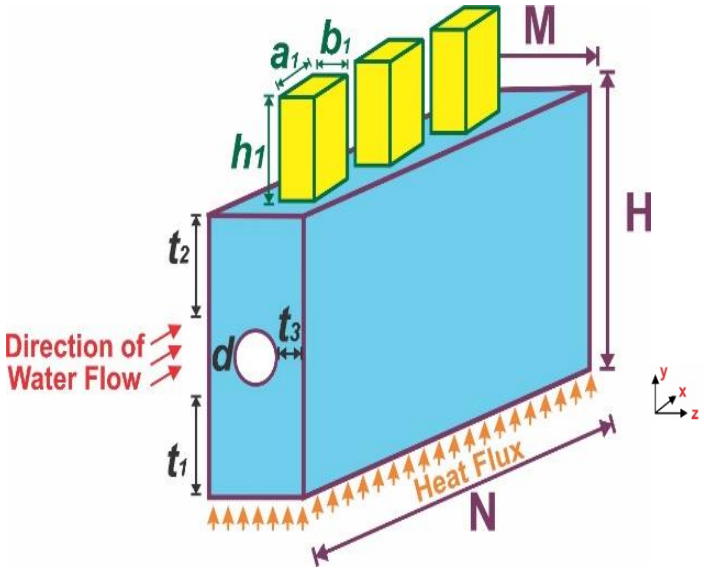

Figure 2: Unit cell computational domain

Figure 2 has circular cooling channel of diameter d and solid rectangular micro-fins of external sides a_1 and b_1, and external height h_1. On the bottom surface of a micro heat sink made of a highly conductive solid aluminium material with a conductivity of 202.4 $k(Wm^{-1}K^{-1})$, a high-density heat flux, q'' is applied. The rectangular fins are placed on a microchannel bottom with circular flow channel. The inlet and temperatures are T_{in} and T_{out} for all the configurations studied.

The three rows and forms of rectangular solid fins are centrally mounted on the unit cell microchannels (Achanta, 2003; Yaghoubi and Velayati, 2005; Adewumi *et al*., 2013), as shown in Figures 1 and 2. The external sides $l_1 \times b_1 \times h_1$ of the rectangular micro fin are $a_1 = 40\ \mu m$ and b_1 is 20 μm, while the external height h_1 is 40 μm. The aspect ratio of the vertical solid rectangular fins $\left(\frac{h_1}{b_1}\right)$ is 2 and falls within the manufacturing constraints in Eqn. (9). The unit cell microchannel heat sink with solid rectangular fins is inserted into the computational domain and fluid (water) is allowed to flow through the microchannel heat sink, the water removes the heat deposited at the bottom of the microchannel. The conjugate heat transfer method was employed to combine the convective heat transfer in the liquid with heat conduction in the solid substrate.

A. Design variables and manufacturing constraints

The solid substrate has fixed axial length N, height H and width M, resulting in a fixed elemental volume v_el, as t_1, t_2 and d_h varies, subject to manufacturing constraints. The ratio of solid volume over the total volume is determined as the solid volume fraction, ϕ. The design under consideration has the following design variables and manufacturing limitations.

The constraint on the heat sink elemental unit cell volume is set as

$$v_{el} = N \times H \times M = \text{constant} \quad (1)$$

The combined heat sink with fins has an elemental volume of

$$v_{elcom} = v_{el} + v_{el_{f1}} + v_{el_{f2}} + \cdots v_{el_{fn}} = \text{constant} \quad (2)$$

where, $v_{el_{fn}}$ is the elemental volume and number of rectangular fins attached to the heat sink.

The cross-sectional area of elemental volume is

$$A = H \times M \quad (3)$$

The void fraction or porosity is

$$\phi = \frac{v_c}{v_{elcom}} \quad (4)$$

The manufacturing constraints for micro heat sink are

$$t_1 \geq 50\mu m \quad (5)$$

$$H - (t_1 + a) \geq 50\mu m \quad (6)$$

The external aspect ratio (*AR*) of the heat sink unit structure is

$$AR = \frac{H}{M} \quad (7)$$

Elemental volume of circular channel is

$$v_c = \frac{\pi}{4} d^2 N \quad (8)$$

The aspect ratio of circular fins is subject to the manufacturing constraints in Eqns. (9).

$$0.5 \leq \frac{h_1}{b_1} \leq 4 \quad (9)$$

The elemental volume of rectangular micro-fins is

$$v_{elf} = h_1 a_1 b_1 \quad (10)$$

Micro fins spacing is

$$S_f \geq 50\mu m \quad (11)$$

III. MATHEMATICAL EQUATIONS AND BOUNDARY CONDITIONS

For the cooling fluids, the following are the continuity, momentum, and energy Equations:

$$\nabla.\vec{\bar{v}} = 0 \quad (12)$$

$$\rho(\vec{v}.\nabla\vec{v}) = -\nabla p + \mu\nabla^2\vec{v} \quad (13)$$

$$\rho_f C_{pf}(\vec{v}.\nabla T) = k_f\nabla^2 \mathrm{T} \quad (14)$$

The energy equation for the solid regions is written as

$$k_s\nabla^2 T = 0 \quad (15)$$

The heat flux at the liquid-solid interface is given as

$$k_s \frac{\partial T}{\partial n}\Big|_{wall} = k_f \frac{\partial T}{\partial n}\Big|_{wall} \quad (16)$$

For the fluid at the channel walls, the no-slip boundary condition is specified.

And at the outflow, there is no stress, therefore;

$$\frac{\partial u}{\partial x} = 0, \frac{\partial v}{\partial x} = 0, \frac{\partial w}{\partial x} = 0, \text{ for } x = N,\ t_3 \leq z \leq d + t_3 \text{ and } t_1 \leq y \leq t_1 + d \quad (17)$$

The Reynolds number of the fluid pumped across the combined microchannel is

$$Re_w = \frac{\rho u d_h}{\mu}, \text{ for } x = 0,\ t_3 \leq z \leq t_3 + d \text{ and } t_1 \leq y \leq d + t_1 \quad (18)$$

The fluid inlet velocity is $u_x = u_{in}, v_y = 0, w_z = 0$ and the inlet temperature is

$$T = T_{in}, \text{ for } x = 0,\ t_3 \leq z \leq t_3 + d \text{ and } t_1 \leq y \leq d + t_1 \quad (19)$$

while thermally developed flow is assumed at the outlet, the temperature at outlet is then.

$$T = T_{w,L}, \text{ for } x = N,\ t_3 \leq z \leq t_3 + d \text{ and } t_1 \leq y \leq d + t_1 \quad (20)$$

The thermal conditions assumed for the bottom-side of the heat sink is given as;

$$k_s \frac{\partial T}{\partial y} = -q'', \text{ for } 0 \leq x \leq N,\ 0 \leq z \leq M \text{ and } y = H \quad (21)$$

The global thermal resistance is expressed in dimensionless form by Olakoyejo *et al.* (2012) as follows;

$$R_{min} = \frac{k_f(T_{w,N} - T_{in})}{q''_N} \approx \frac{k_f \Delta T}{q''_N} \quad (22)$$

A. *Solution and numerical method*

The governing Eqns. (12) – (15) were discretised and solved numerically using a finite volume method using commercially available Computational Fluid Dynamics (CFD) software ANSYS FLUENT 18.1. The computational domain was generated using the enclosure tool in ANSYS fluent (Figure 3 a and b) is divided into many control volumes via the finite volume method (Patankar, 2018). The SIMPLE algorithm was utilised to carry out the pressure-velocity coupling, and the momentum and energy equations were computed using the second order upwind method (Gad-el-Hak, 2002; Laermer and Urban, 2003; Chen and Cheng, 2009; Ismail *et al.*, 2009; Ighalo, 2010; Chai *et al.*, 2011). The convergence was established when for the continuity and momentum, and energy equations, the residuals were lower than 10^{-5} and 10^{-9}, respectively.

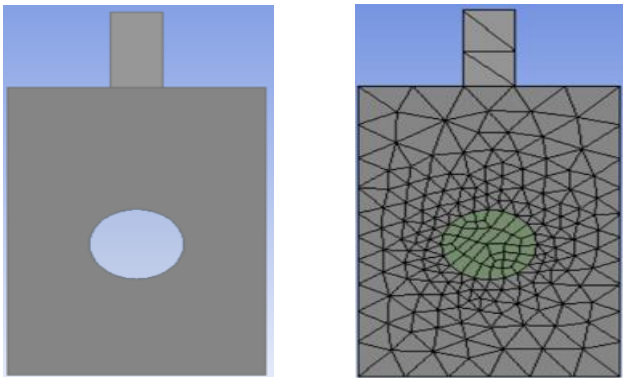

(a) **(b)**

Fig. 3: 3-D microchannel heat sink design (a) using ANSYS design modeler and (b) discretised domain of the micro heat sink

B. *Grid refinement test and code validation*

A grid study is done on the mesh size until an insignificant change in temperature is obtained and the convergence solution. The monitored quantity temperature is

$$\gamma = \left|\frac{(\Delta T_{max})_i - (\Delta T_{max})_{i-1}}{(\Delta T_{max})_i}\right| \leq 0.01 \quad (23)$$

The uniform heat flux used in the simulation and optimisation was employed for the grid refinement test. The combined (hybrid) microchannels with solid fins, are constructed in design modeler environment and discretised using irregular mesh type, hexahedral and tetrahedral computational cell settings.

The geometrical details of the combined microchannel heat sink with solid rectangular fins for the grid refinement test are as depicted in Table 1. The Reynolds number of the fluid (water) pumped across the microchannel axial length is $Re_w = 500$ and the mesh sizes are progressively increased until the monitored quantity of outlet wall temperature of less than 1%. Further grid refinement shows negligible change in the wall temperature (Table 2). For reliability, reduced computational expenses and time, the mesh with nodes and elements chosen for the simulation and optimisation for microchannel heat sinks with circular flow channel and solid rectangular fins is 290 819 and 1 033 776. Further grid refinement does not significantly alter the results of numerical analysis.

The CFD code used in this simulation was validated by plotting and comparing the thermal resistance and Bejan number (Be) obtained in the present prediction and model with the results of Olakoyejo *et al*. (2012). The values in the results show excellent agreement, with deviation of less than 1% (Figure 4). The results of the correlation give confidence and accuracy about the numerical process and code used in this present study.

Table 1: Dimensions for grid refinement

M (mm)	t_3 (mm)	t_2 (mm)	d (mm)	h_1 (mm)	a_1 (mm)	b_1 (mm)	N (mm)
0.1	0.032	0.064	0.036	0.40	0.040	0.020	10

Table 2: Grid independent test results for $v_{el} = 0.15\ mm^3, Re_w = 500$

Node	Elements	$T_{max}(K)$	γ
290, 598	1, 032,001	349.13	0
290, 819	1,033,776	349.13	-
290, 852	1,035,703	349.06	0.0363
290, 952	1,038,703	349.09	0.00042

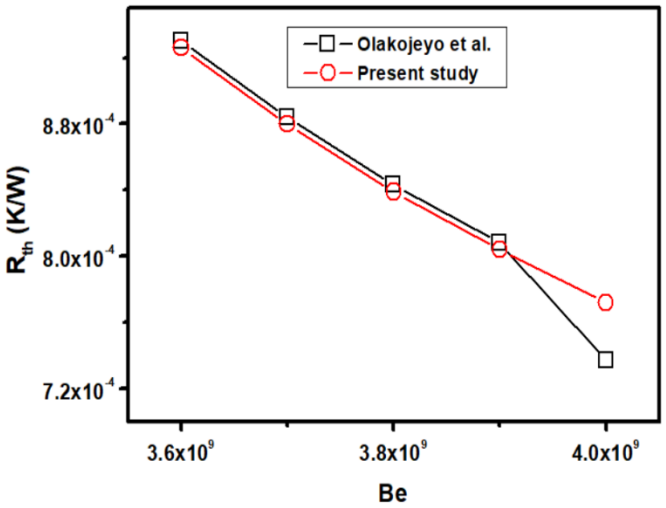

Fig. 4: Numerical code validation: Comparing the thermal esistance with present study

IV. OPTIMISATION TECHNIQUE AND RESULTS PRESENTATION

The key parameters affecting the design were determined, and the optimum conditions that minimise peak temperature were found, using the ANSYS FLUENT 18.1 design exploration optimization tool. The thermal efficiencies of microchannels with a circular cooling channel, but with solid rectangular fins was discussed. Thermal potentials are achieved by performing a numerical simulation and optimisation on the micro heat sink with fins of varying total volume V of 0.15 to 0.17 mm^3 and fixed axial length of $N = 10\ mm$. The design space for the response surface of cooling channel d_h is in the range 0.036 to 0.047 mm, the differences in the thickness from the bottom-side of the combined micro-heat sink and the flow channel is $t_1 \geq 0.05\ mm$, the width M of the combined microchannel varied from 0.01 to 0.115 mm and the difference in thickness t_2 from the flow channel to the top of the combined microchannel is in the range of 0.051 to 0.064 mm, while the thickness between the flow channels t_3 is in the range 0.032 to 0.033 mm.

The range of porosity ϕ is 0.0692 to 0.1009. The constructal solid rectangular fins positioned on the microchannel heat sink with circular cooling channel has three solid fins placed in the positions 5, 5.05 and 5.1 mm respectively, on the micro-heat sink. The total fixed volume of the three (3) micro fins on the unit cell is 96000 μm^3. The heat flux dissipated at the bottom is $2.5 \times 10^6 W/m^2$ and the cooling fluid is in the range of Reynolds number, Re_w, 400 to 500. The inlet temperature of water is 298 K with constant thermos-physical property (Table 3). The minimised global thermal resistance or measure of performance, R_{min} is given in dimensionless form in Eqn. (21).

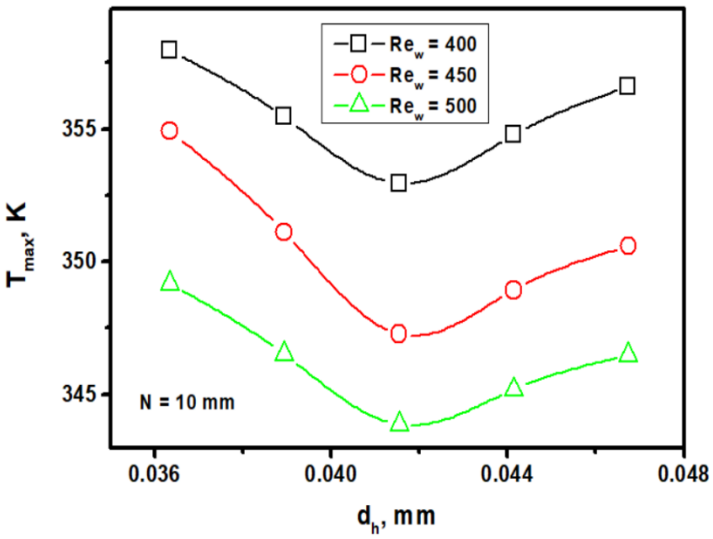

Fig. 5: The effect of diameter on peak temperature

Figure 5 shows the presence of an optimal hydraulic diameter of the microchannel heat sink that minimises the peak temperature. Figure 5 presents the effect of d_h on T_{max}. There was a decrease in peak temperature as the Re_w increases until the diameter corresponding to the minimum temperature is reached. The optimal diameter that gives the minimum temperature at different Reynolds numbers is in the vicinity of 0.0415 mm. The peak temperatures corresponding to the optimal d_h for Reynolds number of 400, 450 and 500 are 352.94, 347.27 and 343.87 KThe micro heat sink cools fastest at highest fluid velocity ($Re_w = 500$) v_{in} of 10.8 m/s. Similarly, the effect of hydraulic diameter $(d_h)_{Opt}$ on peak temperature is presented in Figure 6. $(d_h)_{Opt}$ increases with decrease in T_{max} at the right-hand-side (RHS) of Figures 5 to 8. The peak temperature decreases until the value corresponding to the optimal diameter is reached, after which any further increase in the hydraulic diameter results in increase in T_{max}, as seen in the left-hand-side (LHS) of the curves (Figures 5 to 8). At Reynolds number range of $400 \leq Re_w \leq 500$, the peak temperature diminishes sharply. The combined micro heat sink optimises at 0.0455 mm for the Reynolds number range of $400 \leq Re_w \leq 450$ and 0.0456 mm at $Re_w = 500$. The results show the $(d_h)_{Opt} > d_h$, which is good for the performance of the micro heat sink. The combined microchannel optimises with larger channel width (diameter), as seen in Figures 5 and 8. It means that to increase heat dissipation in the heat sink, more fluid is allowed to flow through the large, optimised channel diameter. In addition, the results show that cooling in the microchannel is achieved by increasing the Reynolds number of fluid and by implication enhanced maximised thermal conductance or minimised thermal resistance.

The peak temperature is plotted against the dimensionless diameter as summarised in Figure 7. As $\frac{d_h}{N}$ increases, T_{max} decreases for the Reynolds number range of

$400 \leq Re_w \leq 500$. The peak temperature decreases by 2.6% as the Reynolds number increases from 400 to 500. The optimal dimensionless diameter is 4.2×10^{-3} for the range of Reynolds number under consideration. More cooling is achieved as the Reynolds number of fluid is increased. In Fig. 8, the plots show that external aspect ratio $\frac{H}{M}$ increases with decrease in T_{max}. The external structure of the micro heat sink continues to adjust in order to give minimum temperature in the entire volume of the combined heat sink. The optimal aspect ratio is about 1.40 for the range of Reynolds number considered and the temperature decreased 357.9 to 343.9 K.

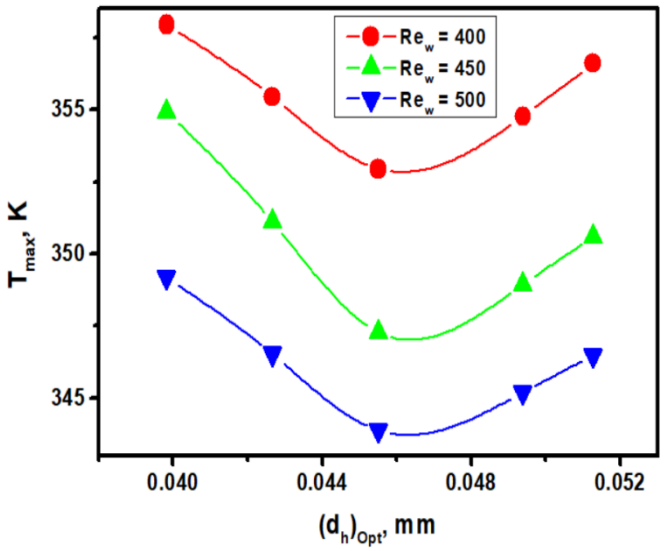

Fig. 6: Effect of optimised hydraulic diameter on peak temperature

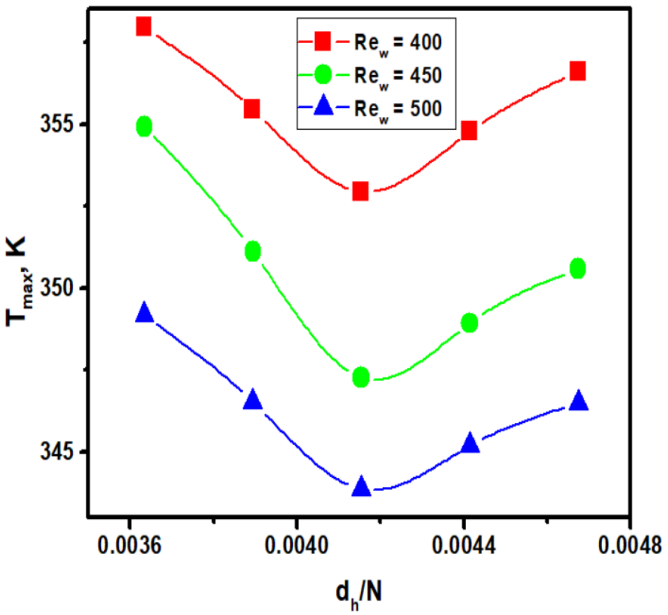

Fig. 7: Effect of dimensionless hydraulic diameter on peak temperature

The effect of Reynolds number Re_w of water on solid material ratio is depicted in Figure 9. It can be seen that the ratio of thicknesses increases with the fluid velocity. The ratio $\frac{2t_3}{t_1}$ increases from 1.33 to 1.64 when the Reynolds number rises from 400 to 500 and after the combined microchannel is optimised, the corresponding optimised thicknesses $\left(\frac{2t_3}{t_1}\right)_{Opt}$ that minimises peak temperature increases from 0.58 to 0.71 at a Reynolds numberof between 400 to 450. And as the Re_w continues to rise from 450 to 500, the graph appears to flatten, as seen in Figure 9. Similarly, the ratios of $\frac{t_1}{t_2}$ and$\left(\frac{t_1}{t_2}\right)_{Opt}$, increases from 0.73 to 089 as the Reynolds number increases in the range $400 \leq Re_w \leq 500$. As it is observed, the values of $\frac{t_1}{t_2}$ and $\left(\frac{t_1}{t_2}\right)_{Opt}$ rises steadily as the fluid velocity increases.

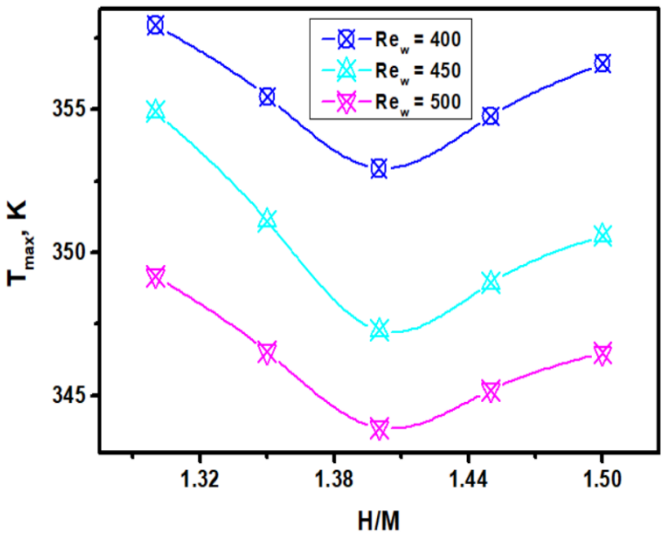

Fig. 8: Influence of external aspect ratio on peak temperature

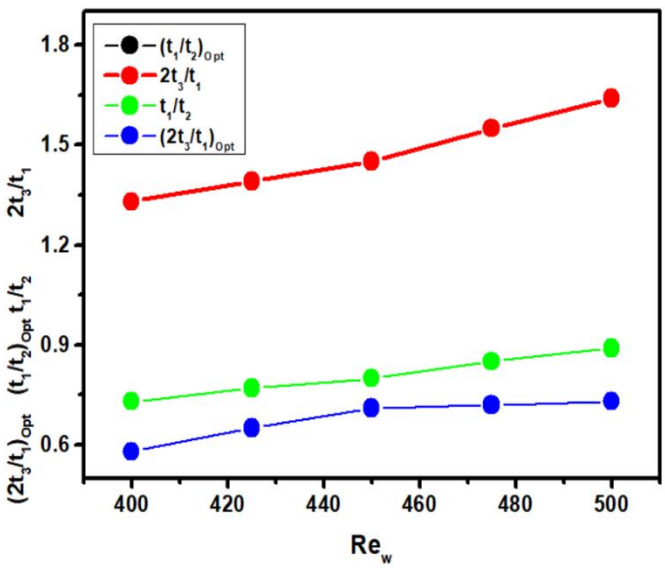

Fig. 9: Effect of Reynolds number on the ratio of thicknesses of solid material substrates

Figure 10 shows minimised temperature as it is affected by the fluid's Reynolds number. For a Reynolds number range of$400 \leq Re_w \leq 500$, the value of $(T_{max})_{min}$ decreases, as seen in Fig. 10. The minimised temperature decreases from

352.94 to 343.89 K as the Reynolds number increases from 400 to 500. As the Reynolds number of the fluid increases by 20%, $(T_{max})_{min}$ decreases by 2.6%, as seen in Figure 10. Therefore, decreasing the minimised temperature, decreases the global thermal resistance, as shown in Figure 11.

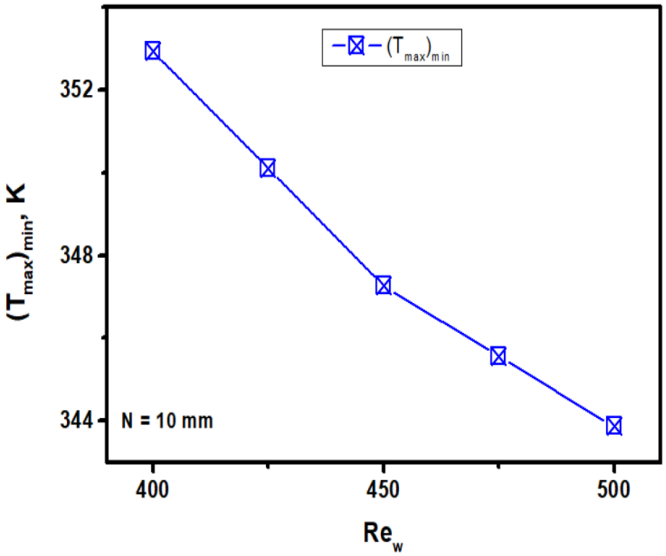

Fig. 10: The effect of Reynolds number on minimised temperature

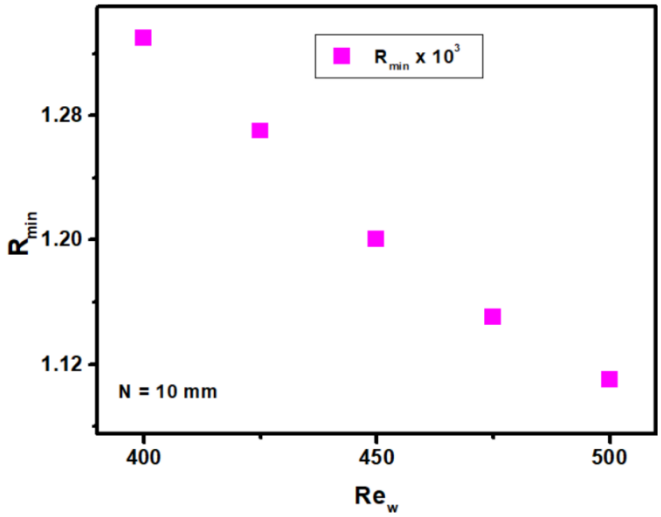

Fig. 11: Effect of Reynolds number of water on global thermal resistance

In Figure 11, the global thermal resistance R_{min} decreases, as Re_w increases. The results show that R_{min} decrease by 16.5% as the Reynolds number of water increases by 20%. More cooling is possible as the fluid velocity increases rapidly.

The performance of microchannel without fins is compared with microchannel with fins and presented in Fig. 12. As Re_w increases, R_{min} decreases. The microchannel without fins decrease by 24% as against the microchannel with fins that decrease by 16.5%, at the same Reynolds number range of 400 to 500.

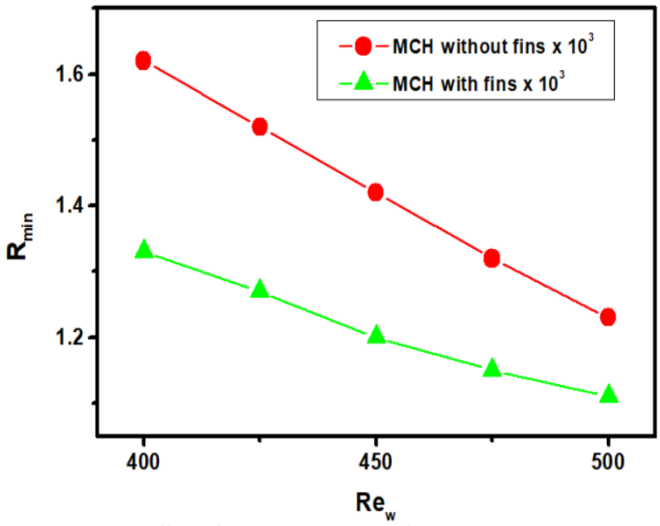

Fig. 12: Effect of Reynolds number of water on global thermal resistance

The results are correlated for the optimised geometry in Eqns. (24) and (25), within a deviation of less than 1% as follows:

$$R_{min} = \alpha Re_w^{-1.232} \text{(Microchannel without fins)} \quad (24)$$

$$R_{min} = \beta Re_w^{-0.874} \text{(Microchannel with fins)} \quad (25)$$

The correlation constants α and β, are 2.61 and 0.263 respectively.

Figures 13 and 14, show the influence of Re_w on the pump power (PP) of the microchannel. As the fluid velocity increases, the pump power requirement of the microchannel increases. The pumping power defines the economy viability and energy demand of the system. The lower the pump power the better. Therefore, increasing the velocity of the fluid results in increased PP. The PP employed to drive the water through the entire volume of the microchannel is expressed by

$$PP = v_{in} A_c \Delta P \quad (26)$$

where v_{in} is the inlet fluid velocity, A_c is the area of the cooling channel and ΔP is the pressure drop across the entire length of the microchannel.

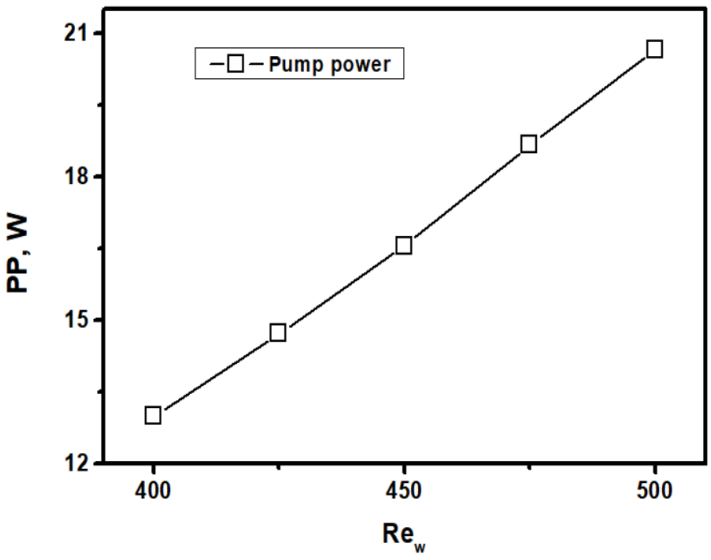

Fig. 13: Influence of Reynolds number on pumping power

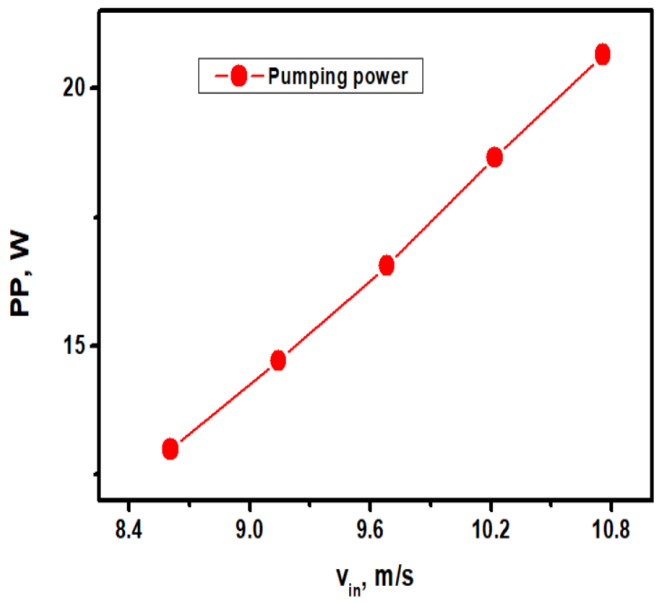

Fig. 14: Influence of velocity of fluid on pump power

Figures 13 and 14 show that as the Reynold number of fluid and velocity increases by 20%, the PP of microchannel with fins increases by 37.1%. The pumping power increases when the Reynolds number and velocity of fluid increases. It is observed that at low Re_w the PP is low, which is accompanied by low cooling in the micro heat sink. But at high Re_w, the PP increases with equivalent increase in cooling in the combined microchannel heat sink, as seen in Figures 13 and 14. The result and trend agreed with what was reported by Adewumi *et al*. (2013).

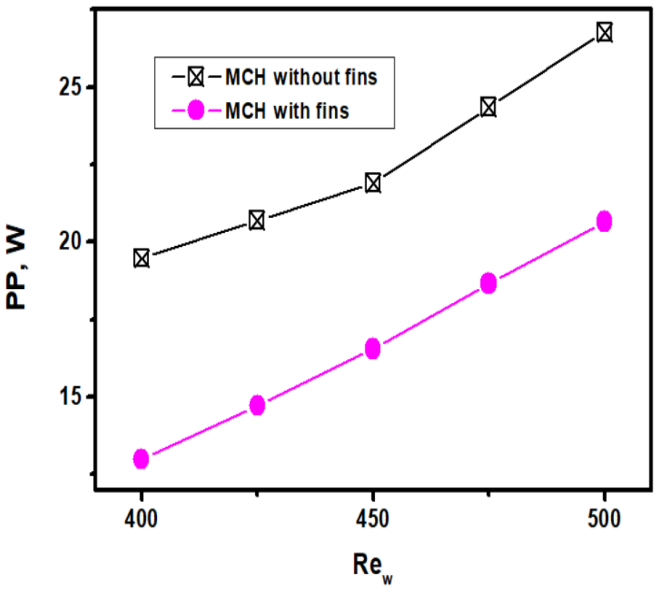

Fig. 15: Influence of Reynolds number on pumping power

Figure 15 shows the effect of Re_w on the pumping power of finless and finned micro heat sinks, as the Reynolds number of the fluid increases, the PP increases, as expected. The trend shows that the micro heat sink without fins has the higher PP compared to the combined microchannel with fins. The Pump power PP is correlated with the Reynolds number Re_w with the deviation of 3% between the values in Eqns. (27) and (28) as

$$PP = \rho Re_w^{1.44} \quad \text{(Microchannel without fins)} \qquad (27)$$

$$PP = \gamma Re_w^{2.144} \quad \text{(Microchannel with fins)} \qquad (28)$$

The correlations are correlated with correlation constants ρ and γ of values 3.39×10^{-3} and 3.43×10^{-5}.

V. CONCLUSION

This paper presents a numerical simulation of combined microchannel heat sink equipped with rectangular solid fins. A fixed volume of micro heat sink with rectangular micro fins having fixed axial length is simulated to remove excessive heat generated from heat flux intensity at the bottom-side of the heat sink. The range of Re_w of fluid (water) applied across the micro heat sink is 400 to 500 with constant thermo-physical properties. The cross-sectional shape of the structure is adjusted until optimise variables that corresponds with the minimised temperature is achieved. The optimisation results showed that as the Re_w increases, the temperature diminishes across the microchannel structure. The higher the velocity of the fluid the better the cooling capabilities.

The optimised values and minimum temperatures are reached at each fluid velocity applied. The micro heat sink optimises well and corresponds to the applied Re_w. It was observed from the study that despite the increase in heat transfer area occasioned by additional vertical rectangular fins, the combined heat sink with solid rectangular vertical fins in comparison with the heat sink without fins has lower resistance, and there is an optimum spacing in the vertical fins and flow channel that corresponds to minimum global thermal resistance or maximum global thermal conductance in the combined microchannels with rectangular fins for a given bottom surface area $M \times N$.

The pumping power PP of the configuration under consideration is calculated and results show that PP increases with Re_w. The combined microchannel with solid rectangular fins consumes lesser energy and more economically viable than the finless heat sink. The constructal technique deployed in the geometric design of combined microchannel heat sink with rectangular solid fins proved exceptional useful in improving the heat transfer properties of the micro heat sink and performed better than the traditional micro heat sink without fins. The study is recommended for cooling microelectronic and microelectromechanical (MEM) devices.

ACKNOWLEDGMENT

The author appreciates the support of Modibbo Adama University, Yola and University of Cape Town (UCT), South Africa for the facilities used during the research.

AUTHOR CONTRIBUTIONS

This paper is the exclusive work of the authors. The concept and every detail in this paper is the original work of the author.

ETHICS

There are no ethical issues or conflict of interest as regards this paper.

REFERENCES

Achanta, V.S. (2003). An experimental study of end wall heat transfer enhancement or flow staggered non-conducting pin fin arrays. Unpublished PhD Thesis, Department of Mechanical Engineering, Texas A & M University, U.S.A.

Adewumi, O.O.; T. Bello-Ochende and J.P. Meyer. (2013). Constructal design of combined microchannel and micro pin fins for electronic cooling. International Journal of Heat and Mass Transfer, 66: 315–323. doi:10.1016/j.ijheatmasstransfer.2013.07.039.

Azoumah, Y.; P. Neveu and N. Mazet. (2007). Optimal design of thermochemical reactors based on constructal approach. AIChE Journal, 53(5): 1257–1266. doi:10.1002/aic.11152.

Bejan, A. (1993). Heat transfer. New Jersey: John Wiley & Sons.

Bejan, A. (2016). Advanced Engineering Thermodynamics. 4th edn. Hoboken: John Wiley & Sons.

Bejan, A. and Dan, N. (1999). Two constructal routes to minimal heat flow resistance via greater internal complexity. Journal of Heat Transfer, 121(1): 6–14. doi:10.1115/1.2825968.

Bejan, A. and Fautrelle, Y. (2003). Constructal multi-scale structure for maximal heat transfer density. Acta Mechanica, 163(1–2)" 39–49. doi:10.1007/s00707-003-1008-3.

Bejan, A. and Lorente, S. (2006). Design with Constructal Theory. International Journal of Engineering Education, 22(1): 140–147.

Bejan, A.; L.A.O. Rocha and S. Lorente. (2000). Thermodynamic optimization of geometry: T- and Y-shaped constructs of fluid streams. International Journal of Thermal Sciences, 39(9–11): 949–960. doi:10.1016/S1290-0729(00)01176-5.

Bello-Ochende, T.; O.T. Olakoyejo; J. P. Meyer; A. Bejan and S. Lorente. (2013). Constructal flow orientation in conjugate cooling channels with internal heat generation. International Journal of Heat and Mass Transfer, 57(1): 241–249. doi:10.1016/j.ijheatmasstransfer.2012.10.021.

Bello-Ochende, T.; J.P. Meyer and A. Bejan. (2010). Constructal multi-scale pin-fins. International Journal of Heat and Mass Transfer, 53(13–14): 2773–2779. doi:10.1016/j.ijheatmasstransfer.2010.02.021.

Bello-Ochende, T.; J.P. Meyer and O.I. Ogunronbi. (2011). Constructal multiscale cylinders rotating in cross-flow. International Journal of Heat and Mass Transfer, 54(11–12): 2568–2577. doi:10.1016/j.ijheatmasstransfer.2011.02.004.

Cetkin, E. (2010). The natural emergence of vascular design with turbulent flow. Unpublished MSc thesis, Duke University, USA.

Chai, L. *et al*. (2011). Numerical simulation of fluid flow and heat transfer in a microchannel heat sink with offset fan-shaped reentrant cavities in sidewall. International Communications in Heat and Mass Transfer, 38(5): 577–584. doi:10.1016/j.icheatmasstransfer.2010.12.037.

Chen, C.; S. Yang and M. Pan. (2021). Microchannel structure optimization and experimental verification of a plate heat exchanger. International Journal of Heat and Mass Transfer, 175: 121385. doi:10.1016/j.ijheatmasstransfer.2021.121385.

Chen, C.L. and Cheng, C.H. (2009). Numerical study of the effects of lid oscillation on the periodic flow pattern and convection heat transfer in a triangular cavity. International Communications in Heat and Mass Transfer, 36(6): 590–596. doi:10.1016/j.icheatmasstransfer.2009.03.006.

Díez, L.I.; S. Espatolero; C. Cortes and A. Campo. (2010). Thermal analysis of rough micro-fins of variable cross-section by the power series method', International Journal of Thermal Sciences, 49(1): 23–35. doi:10.1016/j.ijthermalsci.2009.05.013.

Fan, Y. and Luo, L. (2008). Recent applications of advances in microchannel heat exchangers and multi-scale design optimization', Heat Transfer Engineering, 29(5): 461–474. doi:10.1080/01457630701850968.

Gad-el-Hak, M. (2002). The MEMS Handbook, The MEMS Handbook. Taylor & Francis. doi:10.1201/9780429103872.

Gupta, D.; P. Saha and S. Roy. (2021). Computational analysis of perforation effect on the thermo-hydraulic performance of micro pin-fin heat sink. International Journal of Thermal Sciences, 163: 106857. doi:10.1016/j.ijthermalsci.2021.106857.

Hajialibabaei, M. and Saghir, M.Z. (2022). A critical review of the straight and wavy microchannel heat sink and the application in lithium-ion battery thermal management. International Journal of Thermofluids, 14: 100153. doi:10.1016/j.ijft.2022.100153.

Han, Y.; Y. Liua; M. Liaa and J. Huanga. (2012). A review of development of micro-channel heat exchanger applied in air-conditioning system. in Energy Procedia. Elsevier, 148–153. doi:10.1016/j.egypro.2011.12.910.

He, Z.; Y. Yan and Z. Zhang. (2021). Thermal management and temperature uniformity enhancement of electronic devices by micro heat sinks: A review. Energy, 216: 119223. doi:https://doi.org/10.1016/j.energy.2020.119223.

Ighalo, F.U. (2010). Optimisation of microchannels and micro pin-fin heat sinks with computational fluid dynamics in combination with a mathematical optimisation algorithm. Unpublished MSc. Thesis, Mechanical and Aeronautical Engineering, University of Pretoria, South Africa.

Ismail, L.S.; C. Ranganayakulu and R.K. Shah. (2009). Numerical study of flow patterns of compact plate-fin heat exchangers and generation of design data for offset and wavy fins', International Journal of Heat and Mass Transfer, 52(17–18): 3972–3983. doi:10.1016/j.ijheatmasstransfer.2009.03.026.

John, T.J.; B. Mathew and H. Hegab. (2010). Parametric study on the combined thermal and hydraulic performance of single phase micro pin-fin heat sinks part I: Square and circle geometries', International Journal of Thermal Sciences, 49(11): 2177–2190. doi:10.1016/j.ijthermalsci.2010.06.011.

Kern, D.Q. and Kraus, A.D. (1972) Extended surface heat transfer. New York: McGraw-Hill.

Khan, M.N.; M.N. Karimi and M.O. Qidwai. (2022). Effect of circular perforated pin fin on heat transfer and fluid flow characteristics of rectangular microchannel heat sink. Numerical Heat Transfer, Part A: Applications, 1–15. doi:10.1080/10407782.2022.2101809.

Kim, D.; S.J. Kim and A. Ortega. (2004). Compact modeling of fluid flow and heat transfer in pin fin heat sinks. Journal of Electronic Packaging, Transactions of the ASME, 126(3): 342–350. doi:10.1115/1.1772415.

Koşar, A.; C. Mishra and Y. Peles. (2005). Laminar flow across a bank of low aspect ratio micro pin fins. Journal of Fluids Engineering, Transactions of the ASME, 127(3): 419–430. doi:10.1115/1.1900139.

Koşar, A. and Peles, Y. (2006). Thermal-hydraulic performance of MEMS-based pin fin heat sink', Journal of Heat Transfer, 128(2): 121–131. doi:10.1115/1.2137760.

Kulkarni, R.S. (2005). Infusion of Robustness into the Product Platform Constructal Theory Method. Unpublished MSc Thesis, Department of Mechanical Engineering, Georgia Institute of Technology, USA.

Laermer, F. and Urban, A. (2003). Challenges, developments and applications of silicon deep reactive ion etching. in Microelectronic Engineering. Elsevier 349–355. doi:10.1016/S0167-9317(03)00089-3.

Naphon, P. and Sookkasem, A. (2007). Investigation on heat transfer characteristics of tapered cylinder pin fin heat sinks', Energy Conversion and Management, 48(10), pp. 2671–2679. doi:10.1016/j.enconman.2007.04.020.

Olakoyejo, O.T.; T. Bello-Ochende and J.P. Meyer. (2012). 'Constructal conjugate cooling channels with internal heat generation', International Journal of Heat and Mass Transfer, 55(15–16), pp. 4385–4396. doi:10.1016/j.ijheatmasstransfer.2012.04.007.

Patankar, S. V. (2018). Numerical Heat Transfer and Fluid Flow. CRC Press. doi:10.1201/9781482234213.

Pramanick, A.K. (2007). Natural Philosophy of Thermodynamic Optimization. Unpublished PhD. Thesis, Department of Mechanical Engineering and Materials Science, Duke University, Durham, USA.

Qiu, J.; J. Zhou; Q. Q. Zhao; H. Qin and X. Chen. (2021). Numerical investigation of flow boiling characteristics in cobweb-shaped microchannel heat sink. Case Studies in Thermal Engineering, 28: 101677. doi:10.1016/j.csite.2021.101677.

Reis, A.H. (2006). Constructal theory: From engineering to physics, and how flow systems develop shape and structure. Applied Mechanics Reviews. American Society of Mechanical Engineers Digital Collection: 269–282. doi:10.1115/1.2204075.

Reis, A.H. (2009). Constructal Theory--Complex flow structures in engineering and in Nature. in Conferência Nacional em Mecânica de Fluidos, Termodinâmica e Energia, 1–17.

Rocha, L.A.O.; S. Lorente and A. Bejan. (2002). Constructal design for cooling a disc-shaped area by conduction. International Journal of Heat and Mass Transfer, 45(8): 1643–1652. doi:10.1016/S0017-9310(01)00269-1.

Rocha, L.A.O.; E. Lorenzini and C. Biserni. (2005). Geometric optimization of shapes on the basis of Bejan's Constructal theory. International Communications in Heat and Mass Transfer, 32(10): 1281–1288. doi:10.1016/j.icheatmasstransfer.2005.07.010.

Ryu, J.H.; D.H. Choi and S.J. Kim (2003). Three-dimensional numerical optimization of a manifold microchannel heat sink. International Journal of Heat and Mass Transfer, 46(9): 1553–1562. doi:10.1016/S0017-9310(02)00443-X.

Salimpour, M.R.; M. Sharifhasan and E. Shirani. (2011). Constructal optimization of the geometry of an array of micro-channels. International Communications in Heat and Mass Transfer, 38(1): 93–99. doi:10.1016/j.icheatmasstransfer.2010.10.008.

Siu-Ho, A.. W. Qu and F. Pfefferkorn. (2007). Experimental study of pressure drop and heat transfer in a single-phase micropin-fin heat sink. Journal of Electronic Packaging, Transactions of the ASME, 129(4): 479–487. doi:10.1115/1.2804099.

Tuckerman, D.B. and Pease, R.F.W. (1981). High-Performance Heat Sinking for VLSI. IEEE ELECTRON DEVICE LETTERS, 2(5): 126–129. doi:0193-8576/81/0500-0l26$00.75 0 1981 IEEE.

Vilarrubí, M.; S. Riera; M. Ibanez; M. Omri; G. Lagun; L. Frechette and J. Barra. (2018). Experimental and numerical study of micro-pin-fin heat sinks with variable density for increased temperature uniformity. International Journal of Thermal Sciences, 132: 424–434. doi:10.1016/j.ijthermalsci.2018.06.019.

Wu, W.; L. Chen and F. Sun. (2007). Heat-conduction optimization based on constructal theory', Applied Energy, 84(1): 9–47. doi:10.1016/j.apenergy.2006.04.006.

Yaghoubi, M. and Velayati, E. (2005). Undeveloped convective heat transfer from an array of cubes in cross-stream direction. International Journal of Thermal Sciences, 44(8): 756–765. doi:10.1016/j.ijthermalsci.2005.02.003.

Yeh, R.H. (1997). An analytical study of the optimum dimensions of rectangular fins and cylindrical pin fins. International Journal of Heat and Mass Transfer, 40(15): 3607–3615. doi:10.1016/s0017-9310(97)00010-0.

Zhou, S.; L. Chen. and F. Sun. (2007). Constructal entropy generation minimization for heat and mass transfer in a solid-gas reactor based on triangular element. Journal of Physics D: Applied Physics, 40(11): 3545–3550. doi:10.1088/0022-3727/40/11/044.